*Desalination and Water Treatment*
www.deswater.com
doi: 10.5004/dwt.2023.29823

304 (2023) 219–227
August

# Effect of NaCl on the decolorization and kinetic performance in the chitosan-gelatin composite copper polymer/$H_2O_2$ system

Jie Wang, Xueyan Wang*

*School of Textile Science and Engineering, Xi'an Polytechnic University, 19 Jinhua South Road, Xi'an, Shaanxi 710048, China, emails: wangxueyan815@126.com (X. Wang), 2313269191@qq.com (J. Wang)*

Received 24 February 2023; Accepted 23 July 2023

**ABSTRACT**

To study the effect of salt on decolorization in reactive dyeing wastewater, a chitosan-gelatin composite copper polymer (CG) was prepared as a catalyst, and its structure was characterized by scanning electron microscopy, energy-dispersive X-ray spectroscopy, and Fourier-transform infrared spectroscopy. With the help of CG and $H_2O_2$, a heterogeneous Fenton catalytic system was created, and it was then used to decolorize simulated reactive dyeing effluent. The decolorization effect of C.I. Reactive Blue 19 (RB19) in the CG/$H_2O_2$ catalytic system was studied with and without NaCl. The effects of the initial pH of the decolorization solution, NaCl, and temperature on the decolorization rate and decolorization kinetic properties of RB19 were investigated. The results show that the catalytic decolorization system containing NaCl has a good decolorization effect in a wide range of neutral and alkaline pH values, and the decolorization rate of the CG/$H_2O_2$ catalytic system on the simulated RB19 dyeing wastewater increases with increasing pH value in the pH range of 5~10 and with increasing NaCl concentration. At 50°C for 30 min under neutral and alkaline conditions, the decolorization rate of simulated RB19 dyeing wastewater by CG/$H_2O_2$ catalytic system reaches more than 90%. In the CG/$H_2O_2$ catalytic system, the kinetic models of the catalytic decolorization system with and without NaCl accord with the pseudo-second-order kinetic model. The decolorization rate constant and the initial decolorization rate with NaCl in the dyeing wastewater are more than 3.9 times higher than those recorded without NaCl. The half decolorization time of dyeing wastewater containing NaCl is at least 74% shorter than that of dyeing wastewater without NaCl at the same decolorization temperature.

*Keywords:* Dyeing wastewater; Decolorization; NaCl; Heterogeneous Fenton-like catalyst; Kinetics

## 1. Introduction

Covalent bonds can be created when reactive colors react with fibers. Therefore, the fabrics dyed with reactive dyes have excellent color fastness. Reactive dyes are the most popular dyes for dying cellulose fibers (like cotton) [1]. Water-soluble sulfonic acid groups or carboxylic acid groups are included in the structure of reactive dyes, allowing them to dissolve in water and exist as anions in the dye bath. The surface of cellulose fiber is also electronegative in the dye baths, which is not conducive to the adsorption and dyeing of dyes, resulting in a low dyeing rate and color fixation rate [2,3]. As a result, a large of salts like NaCl and $Na_2SO_4$ are often added to offset the electrostatic repulsion between reactive dye and fiber when dyeing, to improve the dyeing rate. This leads to the high salt content in dyeing wastewater, which increases the burden of wastewater treatment, and the high permeability of salt salinizes the soil of rivers and causes environmental pollution [4].

Wastewater from printing and dyeing processes can be treated using a variety of techniques [5]. Advanced oxidation processes (AOP), one of them, can efficiently treat

* Corresponding author.

dyeing wastewater with complex composition and difficult degradation, which has been recently studied by many scholars [6,7]. Free radicals with strong oxidizing properties can be produced by catalyzing $H_2O_2$ or ozone in AOP, which can degrade organic and inorganic pollutants in wastewater usually by catalyzing $H_2O_2$, and ozone, to produce free radicals with strong oxidizing properties, which can degrade organic pollutants in wastewater into small molecules, and even eventually degrade pollutants into $CO_2$ and $H_2O$ [8]. AOP technique includes the Fenton method [9], wet catalytic oxidation [10], ozone oxidation [11], photocatalysis [12], persulfate oxidation [13], and many others. These studies have proved that AOP has a good decolorization on dyeing wastewater. Due to its ability to circumvent the drawbacks of homogeneous Fenton catalytic system, such as secondary pollution, low pH value of decolorization application, and strict requirements for decolorization conditions, heterogeneous Fenton-like catalyst research is currently attracting the attention of many researcher [14–16]. In this type of catalyst, the metal ligands or supporting elements come in a wide variety. Performances of various heterogeneous Fenton-like catalysts varied. Daud and Hameed [17] studied the decolorization of Acid Red 1 with Fe(III) oxide kaolin catalyst, and a good decolorization was obtained; Guo et al. [18] chelated iron and copper ions on chitosan and used it as a catalyst to treat leachate concentrate, and it achieved 88.24% and 71.45% removal of TOC and COD, respectively. Zhao et al. [19] used magnetite nanoparticles ($Fe_3O_4$-NPs)/orange peel composite as a magnetic heterogeneous Fenton-like catalyst and its removal rate of methyl orange dye wastewater could reach 98% at 20 min. However, in addition to the hard-to-degrade dyestuffs, there are also various auxiliaries, a large number of salts, and other pollutants in the printing and dyeing wastewater, and the presence of these substances will inevitably have some influence on the treatment of wastewater [20]. In dyeing wastewater, NaCl is a chemical that cannot be disregarded. By scavenging hydroxyl radicals (•OH) or aggregate dye molecules in the advanced oxidation process, NaCl has been shown in some studies to slow down the degradation rate of organic pollutants [21,22]. While, other studies have found that high NaCl concentration significantly speed up the dye degradation in the AOP system [23,24]. Therefore, it is worthwhile to investigate how NaCl affects the decolorization of dyeing effluent.

Chitosan gelatin composite copper polymer (CG) was prepared by our research group, and the CG/$H_2O_2$ heterogeneous Fenton system was constructed. It was applied to the treatment of C.I. Reactive Red 24 simulated dyeing wastewater, and a good decolorization was obtained [25]. In this experiment, the decolorization of C.I. Reactive Blue 19 (structure as in Fig. 1) in the catalyst CG/$H_2O_2$ system was studied with and without NaCl. The effect of electrolyte NaCl in dyeing wastewater on the decolorization ratio and decolorization kinetic performance of the catalytic system was studied to understand whether the catalytic system is suitable for the decolorization of NaCl-containing reactive actual dyeing wastewater.

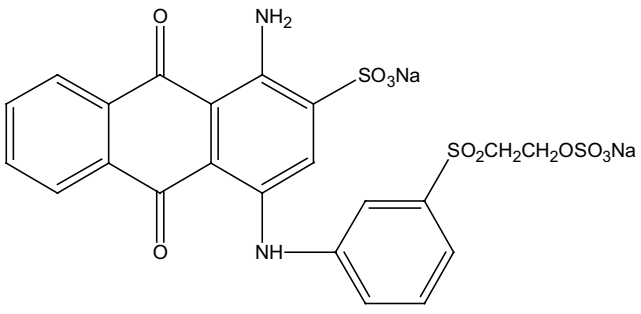


Fig. 1. Structure of C.I. Reactive Blue 19.

## 2. Experimental set-up

### 2.1. Reagents and instruments

C.I. Reactive Blue 19 (RB19) used for this study was supplied by Zhejiang Runtu Co., Ltd., (Zhejiang, China), which was directly applied without further purification. The gelatin copper used in this study was homemade [26,27]. The 30% $H_2O_2$ and all other reagents were of analytical grade and were purchased from Xi'an Chemical Reagent Co., Ltd., (Xi'an, China).

### 2.2. Preparation of the catalyst CG

Firstly, chitosan was dissolved in a 1% acetic acid solution and stirred for 1 h at 60°C to make it dissolve completely. Then gelatin copper solution was slowly added to the dissolved chitosan solution (the mass ratio of chitosan to gelatin copper was 1:30) and stirred for 30 min at 50°C. At last, the precipitate generated by reaction was filtered, fully washed, and baked at 100°C for 3 h to obtain CG.

### 2.3. Decolorization process

The 30% $H_2O_2$ (4 mL/L) and CG (0.4 g/L) were added to the simulated dyeing wastewater which consisted of 0.1 g/L of RB19 and a certain concentration of NaCl (0–18 g/L). The initial pH value of the decolorization solution was adjusted from 5 to 10 with acetic acid or sodium hydroxide. Then the catalytic decolorization was carried out in an HS-type high-temperature computer program-controlled dyeing apparatus from Nantong Hongda Instrument Co., Ltd., (Jiangsu, China) at 50°C for 30 min.

### 2.4. Test of decolorization ratio and decolorization amount

The absorbance of simulated dyeing wastewater was measured with a UV-1900PC type ultraviolet-visible spectrometer from AOE Instrument Co., Ltd., (Shanghai, China) at the wavelength of maximum dye absorption ($\lambda_{max}$, 592 nm) before and after decolorization, respectively. Then the decolorization ratio ($R$) was calculated according to Eq. (1):

$$R(\%) = \left(1 - \frac{A_i \times n}{A_0 \times m}\right) \times 100 \quad (1)$$

where $A_i$ is the absorbance at the maximum absorption wavelength of the simulated dyeing wastewater diluted $n$ times after decolorization, and $A_0$ is the absorbance at the

maximum absorption wavelength of the simulated dyeing wastewater diluted *m* times before decolorization.

The amount of decolorized dye per gram of catalytic material ($q_t$) was calculated according to Eq. (2):

$$q_t = \frac{CV \times R\%}{M} \quad (2)$$

where *C* is the initial concentration of the RB19 of the simulated dyeing wastewater, *V* is the volume of the simulated dyeing wastewater, and *M* is the mass of the added catalyst.

### 2.5. Structural characterization

The microscopic surface morphology of the samples was observed by field emission scanning electron microscopy (SEM, Quanta-450-FEG type, FEI, USA) equipped with energy-dispersive X-ray spectroscopy (EDS). The chemical groups of the samples were examined by Fourier-transform infrared spectroscopy (FTIR, Spectrum Two type, Perkin Elmer Medical Diagnostic Products (Shanghai) Co).

## 3. Results and discussion

### 3.1. Structural characterization of CG

The SEM images of the CG are shown in Fig. 2. From Fig. 2 it can be seen clearly that the surface morphological structure of the CG is uneven, rough, loose, and full of numerous holes. It shows that CG has a large surface area, and it has many adsorption sites. The main elements of CG are C, N, O and Cu, with the Cu content is 7.04 wt.% according to the EDS data in Table 1. This shows that Cu was successfully loaded on CG. The structural of CG are attributed to its adsorption properties for dyes and catalytic properties for $H_2O_2$.

Fig. 3 shows the infrared spectrum of CG, where the broad absorption peak near wave number 3,243 $cm^{-1}$ is due to overlapped absorption peaks of the N–H and O–H stretching vibrations. the absorption peak near wave number 1,644 $cm^{-1}$ is primarily due to C=O and C–N stretching vibration, which is consistent with the characteristic absorption peak of Amide I [28]. The absorption peak near wave number 1,034 $cm^{-1}$ is due to C–O stretching, and the peak near wave number 585 $cm^{-1}$ is due to Cu–O stretching [29–31], indicating the synthesized CG is a composite copper polymer of chitosan and gelatin.

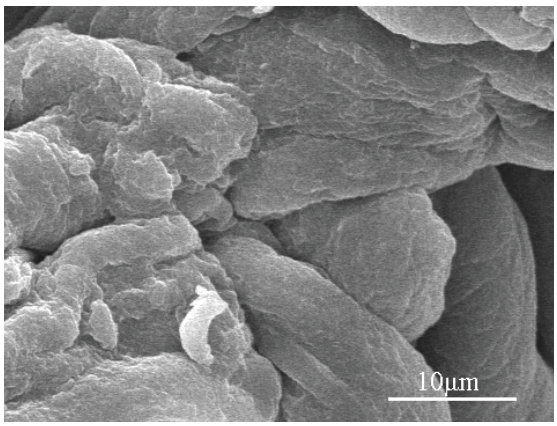


Fig. 2. Scanning electron microscopy images of copper polymer.

### 3.2. Effect of initial pH value of CG/$H_2O_2$ catalytic system on decolorization of simulated dyeing wastewater

0.1 g/L of simulated RB19 dyeing wastewater with and without NaCl (6 g/L) at different pH values were prepared, respectively. Then the decolorization was carried out according to the decolorization process mentioned in 2.3. The decolorization results are shown in Fig. 4.

According to Fig. 4, treating simulated RB19 dyeing wastewater by CG/$H_2O_2$ catalytic system under alkaline conditions can result in a superior decolorization impact because the decolorization ratio of RB19 in the catalytic system improves with the increase in pH value. Classical Fenton reaction uses ferrous ion as the catalyst, which reacts with $H_2O_2$ to produce the Fenton reagent. The reaction is suitable for a strong acid environment with a pH of around 3. In addition, with the production of iron sludge in the reaction process, the decolorization method has limitations [32,33]. However, in this study, a biological complex CG was used as a catalyst to construct a heterogeneous Fenton system with $H_2O_2$. Compared with iron ions, the insoluble copper-based catalyst can adapt to a wider pH range [34,35]. But iron-based catalysts catalyze the decomposition of

Table 1
Mass percentage of major elements in copper polymer (wt.%)

| | Catalyst copper polymer |
|---|---|
| C | 41.23 |
| O | 37.93 |
| N | 13.81 |
| Cu | 7.04 |

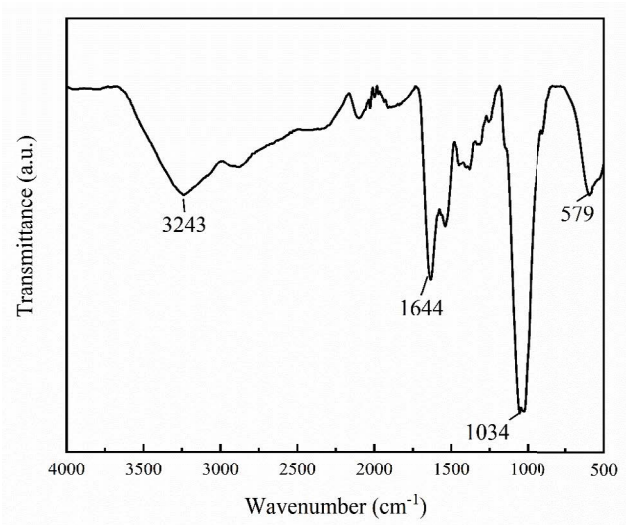


Fig. 3. Fourier-transform infrared spectroscopy image of copper polymer.

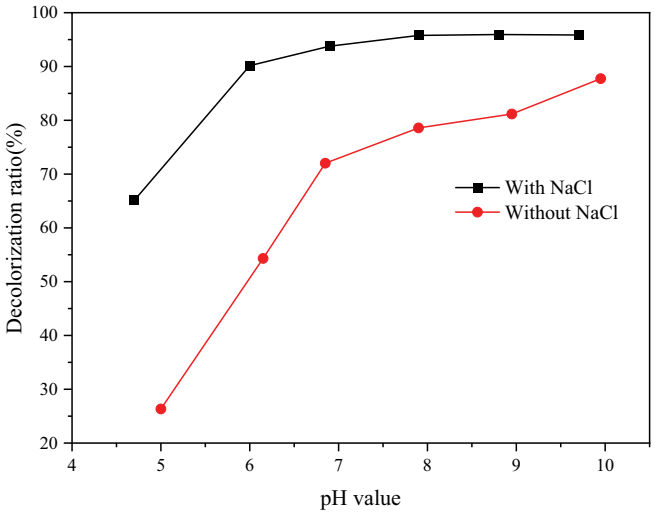


Fig. 4. Effect of initial pH value of simulated dyeing wastewater on decolorization ratio.

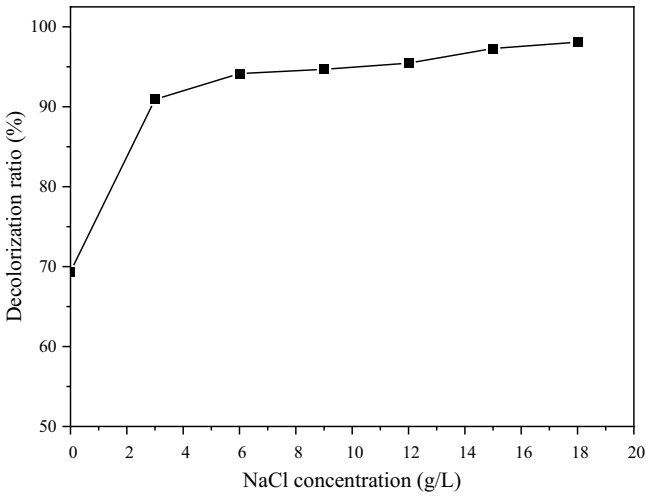


Fig. 5. Effect of NaCl concentration in dyeing wastewater on decolorization ratio.

$H_2O_2$ to produce strong oxidation hydroxyl radicals (•OH), which is the main active substance [36–38]. At higher pH levels, iron ions are less soluble, and iron hydroxide precipitates can even develop. The formation of •OH becomes slow, resulting in the reduction of the degradation rate of organic pollutants in wastewater [39,40]. Therefore, this heterogeneous catalytic system has obvious advantages over the homogeneous Fenton catalytic system.

And it can be also seen from Fig. 4 that under the same pH condition, the decolorization ratio of simulated RB19 dyeing wastewater containing NaCl in the CG/$H_2O_2$ catalytic system is higher than that of simulated dyeing wastewater without NaCl, which shows that the presence of NaCl in dyeing wastewater is beneficial to improve the catalytic decolorization of this system. According to Fig. 4, when the pH value is 7, the decolorization ratios of dyeing wastewater without NaCl and with NaCl reached 70% and 90% at 50°C for 30 min, respectively. It shows that a good decolorization effect can be obtained in a wide range of neutral and alkaline pH values in the NaCl-containing reactive dyeing wastewater.

Due to reactive dyeing, a significant amount of salt must to be added to help dyes adhere to the fiber. Therefore, there must be a lot of salt in reactive dyeing wastewater. Therefore, the CG/$H_2O_2$ catalytic system is very conducive to the decolorization of reactive dyeing wastewater. Subsequently, the pH value of the simulated dyeing wastewater was not adjusted, and the decolorization process was carried out under near neutral conditions.

### *3.3. Effect of NaCl concentration in simulated dyeing wastewater on decolorization*

The simulated dyeing wastewater containing different concentrations of NaCl was decolorized according to the decolorization process mentioned in 2.3. The pH value of the simulated dyeing wastewater was not adjusted. Then the decolorization ratio was measured. The results are shown in Fig. 5.

According to Fig. 5, it can be seen that the decolorization of simulated RB19 dyeing wastewater in the CG/$H_2O_2$ catalytic system increases as the concentration of NaCl increased. When the concentration of NaCl in the simulated RB19 dyeing wastewater was increased from 0 to 3 g/L, the decolorization ratio increased substantially, while the increase of decolorization gradually decreased when the concentration of NaCl was greater than 3 g/L. It indicates that the presence of NaCl in the dyeing wastewater can increase the decolorization rate, which is beneficial to the decolorization of the reactive dyeing wastewater by the catalytic system. This may be because chlorine ions can catalyze the decomposition of $H_2O_2$ in concert with the catalyst CG. The copper ions on the catalyst can complex with chloride ions, and the complex formed facilitates the conversion of Cu(II)→Cu(I), thus accelerating the cycle between Cu(II) and Cu(I), which increases the production of hydroxyl radical (•OH), thereby improving the degradation rate of dyes in dyeing wastewater. On the other hand, chlorine ions may be oxidized by hydroxyl radicals to form reactive chlorine (RCS), which also has oxidizing properties and can oxidatively degrade dyes in dyeing wastewater [41,42]. Therefore, the presence of NaCl in dyeing wastewater will enhance the decolorization effect.

Fig. 6 is the absorption spectrum curve of simulated RB19 dyeing wastewater with NaCl (6 g/L) and without NaCl at different decolorization times. From Fig. 6 it can be seen that the maximum absorption wavelength of RB19 is 592 nm. With an increase in decolorization time, the dye's absorbance at its maximum absorption wavelength rapidly declines or even disappears. It shows that the dye molecules in wastewater are constantly adsorbed and destroyed, and the number of dyes in wastewater decreases [43]. Compared with Fig. 6a and b, it can be found that when the treatment time is the same, the absorbance of simulated RB19 dyeing wastewater with NaCl decreases more than that of simulated RB19 dyeing wastewater without NaCl. The results show that the existence of NaCl in dyeing wastewater is conducive to promoting decolorization, In the presence of NaCl, the ability of CG to adsorb dyes and catalyze the decomposition of

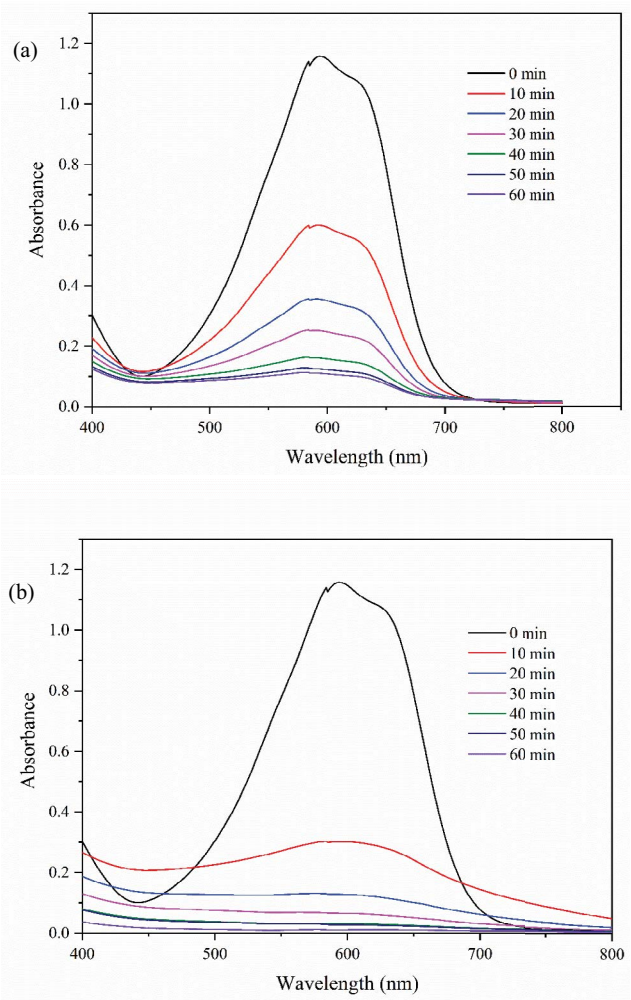


Fig. 6. Absorption spectral curves of simulated dyeing wastewater without NaCl (a) and with NaCl (b) at different decolorization times.

$H_2O_2$ are enhanced, which accelerates the decolorization of wastewater and improves the decolorization rate. However, with the progress of the reaction, $H_2O_2$ is gradually consumed, and the various active substances in the catalytic system are gradually reduced, therefore, the rate of oxidative degradation of dyes gradually decreases, and the destruction rate of dyes gradually decreases. It is quite difficult to completely degrade dyes into carbon dioxide and water.

### 3.4. Effect of different systems on decolorization of simulated dyeing wastewater

Different systems were used to decolorize simulated RB19 dyeing wastewater according to the decolorization process mentioned in 2.3. Decolorization was carried out at different times at 50°C. The results are shown in Fig. 7.

According to Fig. 7, when $H_2O_2$ is used alone to decolorize simulated RB19 dyeing wastewater, the decolorization ratio is very low, and the decolorization ratio is less than 10% at 50°C for 60 min. This is due to the slow decomposition rate of $H_2O_2$ under neutral conditions at 50°C, which

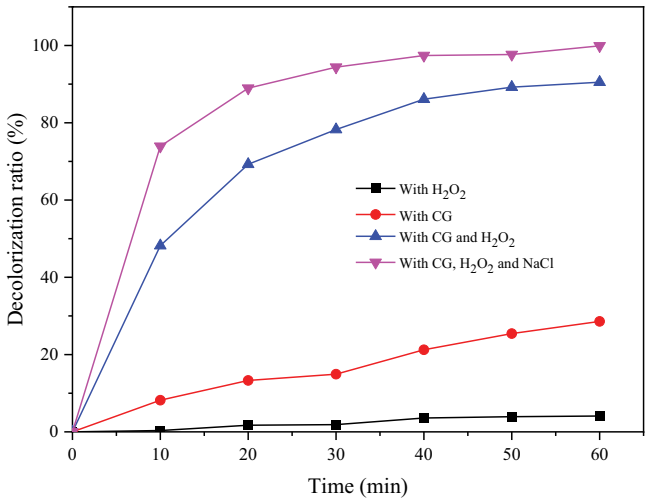


Fig. 7. Decolorization rate of different systems on simulated RB19 dyeing wastewater.

has little decolorization for dyeing wastewater. When the CG is utilized exclusively, the decolorization rate is improved, and the decolorization ratio is nearly 30% under the same conditions. The reason is that CG has a certain adsorption effect on dyes in dyeing wastewater. $H_2O_2$ and CG by themselves cannot achieve a reasonable decolorization rate due to their extremely low decolorization rates. Compared with CG and $H_2O_2$ alone, the decolorization rate of simulated RB19 dyeing wastewater treated by CG/$H_2O_2$ system is improved highly. It demonstrates how CG may effectively degrade the structure of dyes, stimulate the breakdown of $H_2O_2$, release highly active chemicals, and then considerably increase the decolorization rate. Moreover, when CG/$H_2O_2$/NaCl system is used to treat the dyeing wastewater, its decolorization rate is higher than that of the CG/$H_2O_2$ system. It further shows that NaCl can improve the decolorization of the CG/$H_2O_2$ system on simulated RB19 dyeing wastewater to a certain extent in the CG/$H_2O_2$ catalytic system.

### 3.5. Effects of temperature and salt on decolorization kinetics

The decolorization was investigated at 40°C, 50°C, and 60°C with the addition of NaCl (6 g/L) and without the addition of NaCl, and the decolorization amount was tested at different times. The results are shown in Fig. 8.

As can be seen in Fig. 8, the decolorization rate increases significantly with the increase of temperature with or without NaCl. And the decolorization rate with the addition of NaCl was significantly higher than that without the addition of NaCl at the same temperature. The influence of NaCl on the decolorization kinetics performance of the catalytic system is analyzed below.

### 3.6. Dynamic model

#### 3.6.1. Pseudo-first-order

The pseudo-first-order equation is shown in Eq. (3) [44].

$$\frac{dq_t}{dt} = k_1\left(q_e - q_t\right) \tag{3}$$

where $q_t$ is the decolorization amount (mg/g) at $t$ min; $q_e$ is the equilibrium decolorization amount (mg/g); $k_1$ is the first-order kinetic reaction rate constant ($min^{-1}$).

After integrating Eq. (3), and substituting the critical conditions $t = 0$, $q_t = 0$ and $t = t$, $q_t = q_t$, Eq. (4) is obtained.

$$\ln\left(q_e - q_t\right) = \ln q_e - \frac{k_1 t}{R} \tag{4}$$

The data were linearly fitted with t as the independent variable and $\ln(q_e - q_t)$ as the dependent variable. Based on the experimental data obtained in Fig. 8, the pseudo-first-order dynamics fitting is shown in Fig. 9 at different temperatures with and without NaCl. The linear regression coefficients are seen in Table 2.

### 3.6.2. Pseudo-second-order

The pseudo-second-order equation is shown in Eq. (5):

$$\frac{dq_t}{dt} = k_2\left(q_e - q_t\right)^2 \tag{5}$$

where $q_t$ is the decolorization amount (mg/g) at $t$ min; $q_e$ is the equilibrium decolorization amount (mg/g); $k_2$ is the second-order kinetic reaction rate constant (g/(min·mg)).

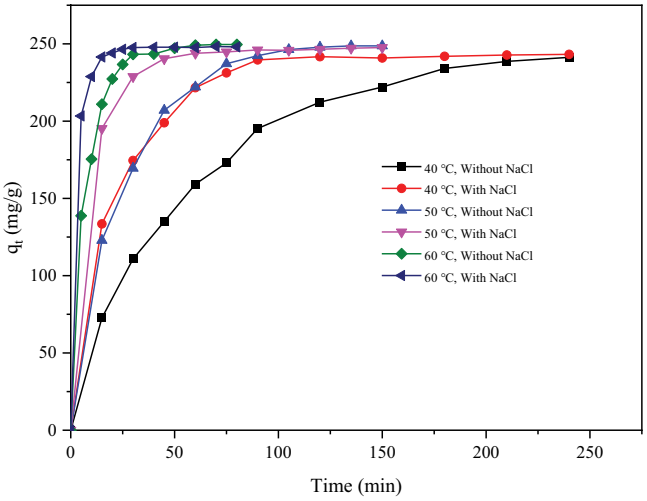


Fig. 8. Decolorization rate curves at different temperatures with and without NaCl.

After integrating Eq. (5), and substituting the critical conditions $t = 0$, $q_t = 0$ and $t = t$, $q_t = q_t$, Eq. (6) is obtained.

$$\frac{t}{q_t} = \frac{1}{k_2 q_e^2} + \frac{t}{q_e} \tag{6}$$

The data were linearly fitted with $t$ as the independent variable and $t/q_t$ as the dependent variable. Based on the experimental data obtained in Fig. 8, the pseudo-second-order dynamics fitting is shown in Fig. 10 at different temperatures with and without NaCl. The linear regression coefficients are seen in Table 2.

As can be seen from Figs. 9, 10, and Table 2, whether there is NaCl or not, the decolorization kinetic model of the simulated RB19 dyeing wastewater is more in line with the pseudo-second-order kinetic model in the CG/$H_2O_2$ catalytic system. The linear fitting coefficients of pseudo-second-order dynamics in all experiments are very high, close to 1. In the case of without NaCl, the decolorization of the simulated RB19 dyeing wastewater can also better accord with the pseudo-first-order kinetic model in the CG/$H_2O_2$ catalytic system. However, in the presence of NaCl, the decolorization of the simulated RB19 dyeing wastewater does not accord with the pseudo-first-order kinetic model in the CG/$H_2O_2$ catalytic system. Therefore, the decolorization kinetics was changed by adding NaCl to the CG/$H_2O_2$ catalytic system. The decolorization rate of the system is directly proportional to the square of the dye concentration in the dyeing wastewater.

### 3.6.3. Dynamic parameters

To further explore the effect of NaCl on the decolorization kinetic performance of the CG/$H_2O_2$ catalytic system, the kinetic parameters of decolorization rate constant, half decolorization time ($t_{1/2}$), and initial decolorization rate ($v_0$) with and without NaCl were compared (Table 3). Because the decolorization system is more in line with the pseudo-second-order kinetic model, the kinetic parameters were calculated by the pseudo-second-order kinetic linear equation. Half decolorization time is the time required to reach half of the equilibrium decolorization amount, represented by $t_{1/2}$. It can reflect the speed of the decolorization rate. When $t = t_{1/2}$, $q_t = q_e/2$ is substituted into Eq. (6), the calculation formula of half decolorization time $t_{1/2}$ (its unit is min.) can be obtained, Eq. (7). Generally, the initial decolorization rate

Table 2
The $R^2$ of the pseudo-first-order model and the pseudo-second-order model

| | Temperature (°C) | Linear regression coefficient $R^2$ | |
|---|---|---|---|
| | | Pseudo-first-order model | Pseudo-second-order model |
| Without NaCl | 40 | 0.99404 | 0.9984 |
| | 50 | 0.98999 | 0.99741 |
| | 60 | 0.96796 | 0.99898 |
| With NaCl | 40 | 0.7534 | 0.99859 |
| | 50 | 0.77193 | 0.99978 |
| | 60 | 0.58917 | 0.9999 |

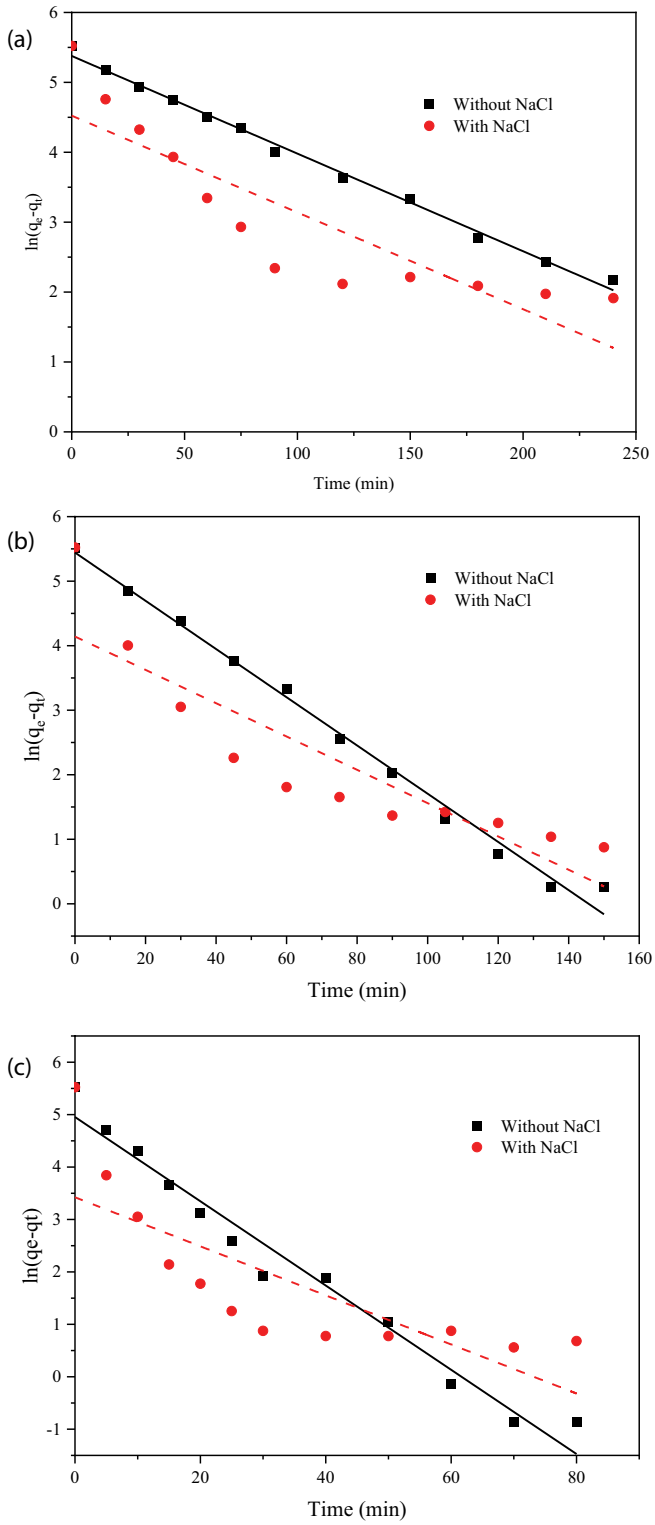


Fig. 9. Linear fitting curve of adsorption pseudo-first-order kinetic model at 40°C (a), 50°C (b), and 60°C (c) with and without NaCl.

(represented by $v_0$, its unit is mg/min.) is directly proportional to the decolorization rate constant and the square of the equilibrium decolorization amount, as shown in Eq. (8) [45].

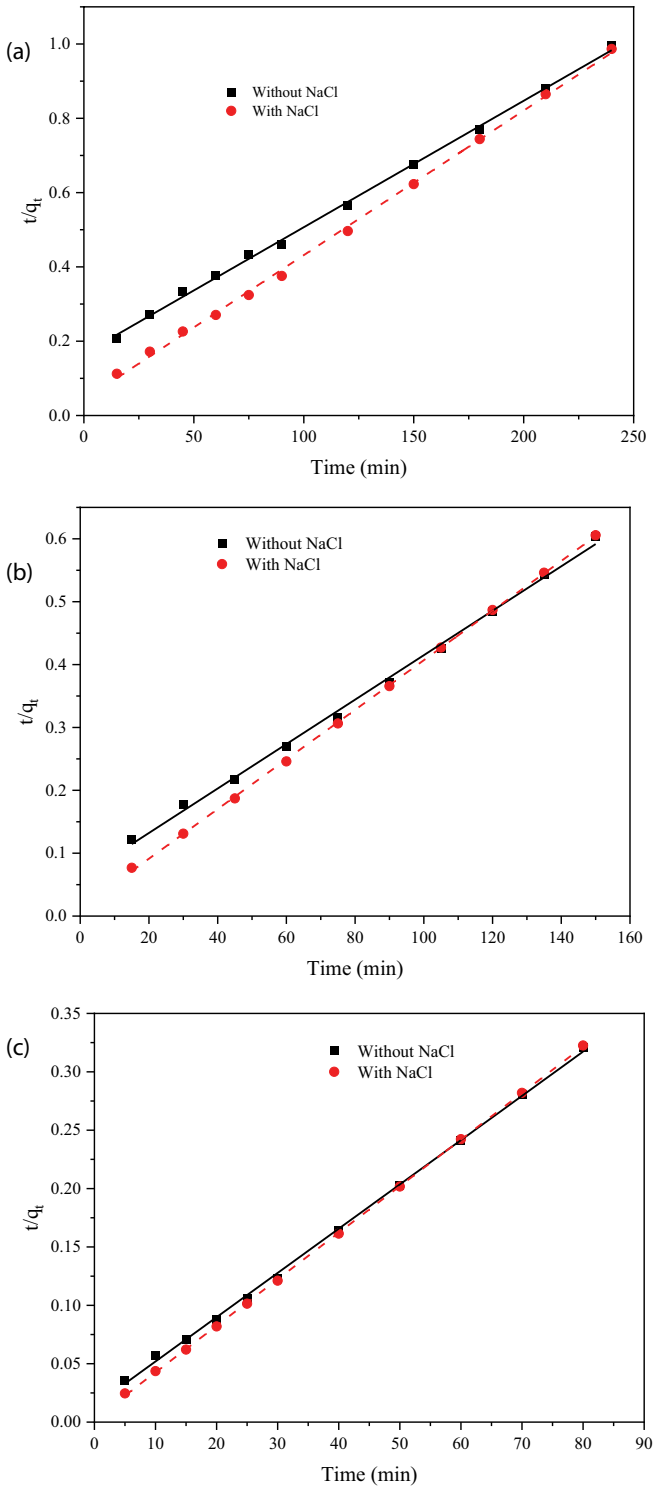


Fig. 10. Linear fitting curve of adsorption pseudo-second-order kinetic model at 40°C (a), 50°C (b), and 60°C (c) with and without NaCl.

$$t_{1/2} = \frac{1}{k_2 \times q_e} \tag{7}$$

$$v_0 = k_2 \times q_e^2 \tag{8}$$

Table 3
Kinetic parameters calculated according to pseudo-second-order dynamic equation

| | Temperature (°C) | $k_2$ (1/(min·mg)) | $t_{1/2}$ (min) | $v_0$ (mg/min) |
|---|---|---|---|---|
| Without NaCl | 40 | $9.61 \times 10^{-5}$ | 41.61 | 6.01 |
| | 50 | $2.60 \times 10^{-4}$ | 15.37 | 16.26 |
| | 60 | $1.14 \times 10^{-3}$ | 3.51 | 71.33 |
| With NaCl | 40 | $3.75 \times 10^{-4}$ (3.90) | 10.65 (0.26) | 23.47 (3.90) |
| | 50 | $1.30 \times 10^{-3}$ (5.00) | 3.09 (0.20) | 81.04 (4.98) |
| | 60 | $5.71 \times 10^{-3}$ (5.01) | 0.7 (0.20) | 357.14 (5.01) |

Values in brackets are the ratio of the corresponding kinetic parameters of decolorization at the same temperature with and without NaCl.

As can be seen from Table 3, with the increase in temperature and the addition of NaCl, the pseudo-second-order kinetic decolorization reaction rate constant $k_2$ and the initial decolorization rate $v_0$ increase, while half decolorization time $t_{1/2}$ decreases. The results show that increasing temperature and adding NaCl are beneficial to increasing the decolorized rate and reducing the decolorized time. The reason for increasing the decolorization rate by increasing temperature is that the decomposition rate of $H_2O_2$ catalyzed by CG increases, releasing more active free radicals like hydroxyl radical (•OH), and the effective collision among dyes, CG, and highly active oxidizing substances increases. Another reason is that the absorption rate of CG towards dyes increases with the increase of temperature, which is also beneficial for improving the decolorization rate [46–48]. It can be seen from Table 3 that under the same decolorization temperature, the decolorization rate constant and initial decolorization rate with NaCl are more than 3.9 times higher than those without NaCl, and the half decolorization time with NaCl is shortened by at least 74% than that without NaCl. NaCl improves the decolorization rate by reducing the electrostatic repulsion between anionic reactive dyes, increasing the adsorption force of dye molecules and their aggregates on the CG, and increasing more dyes adsorb on the surface of the CG, to improve the decolorization rate. But in this decolorization experiment, the concentration of NaCl is 6 g/L, which has little effect on improving the rate of dye adsorption by CG. As a result, the principal mechanism by which NaCl increases the decolorization rate is to promote the decomposition of $H_2O_2$ to produce more highly active oxidation particles, effectively destroy the structure of dyes, and then improve the decolorization rate [49,50]. Therefore, the presence of NaCl in the CG/$H_2O_2$ catalytic system could increase the decolorization rate and reduce the decolorization time.

## 4. Conclusions

The CG/$H_2O_2$ catalytic system was used to decolorize RB19 simulated dyeing wastewater both with and without NaCl. With NaCl, the decolorization rate constant and the initial decolorization rate are more than 3.9 times higher than they would be without it, and a half decolorization time with NaCl is shortened by at least 74% at the same decolorization temperature. Additionally, the NaCl-containing catalytic decolorization system has a good decolorization effect in a wide range of neutral and alkaline pH values (7–10). It indicates that the presence of NaCl in dyeing wastewater is beneficial to improve the decolorization rate and shorten the decolorization time required for decolorization in the CG/$H_2O_2$ catalytic system. So, the catalytic system is especially suitable for the decolorization of reactive dyeing wastewater. The pseudo-second-order kinetic model and the kinetic model of the catalytic decolorization with and without NaCl are in agreement.

## Acknowledgments

This work was supported by the Industrial Research Program of the Technology Board of Shaanxi Province, China (No. 2022GY-164) and by the National Innovation Center of Advanced Dyeing and Finishing Technology, Tai'an, Shandong, China (No. ZJ2021B01).

## References

[1] I. Arslan-Alaton, A review of the effects of dye-assisting chemicals on advanced oxidation of reactive dyes in wastewater, Color. Technol., 119 (2003) 345–353.
[2] N.S.E. Ahmed, The use of sodium edate in the dyeing of cotton with reactive dyes, Dyes Pigm., 65 (2005) 221–225.
[3] A. Khatri, A review on developments in dyeing cotton fabrics with reactive dyes for reducing effluent pollution, J. Cleaner Prod., 87 (2015) 50–57.
[4] K. Srikulkit, P. Santifuengkul, Salt-free dyeing of cotton cellulose with a model cationic reactive dye, Color. Technol., 116 (2000) 398–402.
[5] W. Sun, K. Yang, Discussion on printing and dyeing wastewater treatment methods, IOP Conf. Ser.: Earth Environ. Sci., 514 (2020) 052030, doi: 10.1088/1755-1315/514/5/052030.
[6] A. Babuponnusami, K. Muthukumar, A review on Fenton and improvements to the Fenton process for wastewater treatment, J. Environ. Chem. Eng., 2 (2014) 557–572.
[7] B. Sun, H. Li, X. Li, X. Liu, C. Zhang, H. Xu, X.S. Zhao, Degradation of organic dyes over Fenton-like $Cu_2O$–Cu/C catalyst, Ind. Eng. Chem. Res., 57 (2018) 14011–14021.
[8] M. Muruganandham, R.P.S. Suri, SH. Jafari, M. Sillanpää, G.-J. Lee, J.J. Wu, M. Swaminathan, Recent developments in homogeneous advanced oxidation processes for water and wastewater treatment, Int. J. Photoenergy, 2014 (2014) 164–167.
[9] T. Zhou, X. Lu, J. Wang, F.S. Wong, Y.Z. Li, Rapid decolorization and mineralization of simulated textile wastewater in a heterogeneous Fenton like system with/without external energy, J. Hazard. Mater., 165 (2009) 193–199.
[10] C.S.D. Rodrigues, S.A.C. Carabineiro, F.J. Maldonado-Hódar, L.M. Madeira, Wet peroxide oxidation of dye-containing wastewaters using nanosized au supported on $Al_2O_3$, Catal. Today, 280 (2017) 165–175.
[11] L.P. Wang, Y.J. Mao, Y.C. Guo, E.D. Du, Research on the treatment of dyeing wastewater by heterogeneous catalytic ozonation process, Adv. Mater. Res., 367 (2011) 3793–3796.

[12] L.S. Silva, M.M.M. Gonçalves, L.R. Raddi De Araujo, Combined photocatalytic and biological process for textile wastewater treatments, Water Environ. Res., 91 (2019) 1490–1497.
[13] E. Adar, Removal of Acid Yellow 17 from textile wastewater by adsorption and heterogeneous persulfate oxidation, Int. J. Environ. Sci. Technol., 18 (2021) 483–498.
[14] B. Samir, S. Bakhta, N. Bouazizi, Z. Sadaoui, O. Allalou, F. Le Derf, J. Vieillard, TBO degradation by heterogeneous Fenton-like reaction using Fe supported over activated carbon, Catalysts, 11 (2021) 1456, doi: 10.3390/catal11121456.
[15] S. Hussain, E. Aneggi, S. Maschio, M. Contin, D. Goi, Steel scale waste as a heterogeneous Fenton-like catalyst for the treatment of landfill leachate, Environ. Sci. Pollut. Res. Int., 60 (2021) 11715–11724.
[16] A.S.Y. Liew, S.Y. Nguang, L.J. Minggu, N. Tahir, P.Y. Moh, Graphene oxide incorporated amino-functionalized iron terephthalate composite as a heterogeneous Fenton-like catalyst, J. Chin. Chem. Soc., 68 (2021) 1887–1896.
[17] N.K. Daud, B.H. Hameed, Acid Red 1 dye decolorization by heterogeneous Fenton-like reaction using Fe/kaolin catalyst, Desalination, 269 (2011) 291–293.
[18] C. Guo, X. Qin, R. Guo, Y. Lv, M. Li, Z. Wang, T. Li, Optimization of heterogeneous Fenton-like process with Cu-Fe@CTS as catalyst for degradation of organic matter in leachate concentrate and degradation mechanism research, Waste Manage., 134 (2021) 220–230.
[19] Q. Zhao, C. Zhang, X. Tong, Y. Zou, Y. Li, F. Wei, composite as magnetic heterogeneous Fenton-like catalyst towards high-efficiency degradation of methyl orange, Water Sci. Technol., 84 (2021) 159–171.
[20] H. Xu, B. Yang, Y. Liu, F. Li, C. Shen, C. Ma, Q. Tian, X. Song, W. Sand, Recent advances in anaerobic biological processes for textile printing and dyeing wastewater treatment: a mini-review, World J. Microbiol. Biotechnol., 34 (2018) 165, doi: 10.1007/s11274-018-2548-y.
[21] M.M. El-Fass, N.A. Badawy, A.A. El-Bayaa, The influence of simple electrolyte on the behaviour of some acid dyes in aqueous media, Spectrochim. Acta, Part A, 16 (1995) 458–461.
[22] M. Muthukumar, Studies on the effect of inorganic salts on decolouration of acid dye effluents by ozonation, Dyes Pigm., 62 (2004) 221–228.
[23] S.Y. Yang, Y.X. Chen, L.P. Lou, W.U. Xiao-Na, Involvement of chloride anion in photocatalytic process, J. Environ. Sci., 17 (2005) 761–765.
[24] R. Yuan, S.N. Ramjaun, Z. Wang, J. Liu, Photocatalytic degradation and chlorination of azo dye in saline wastewater: kinetics and AOX formation, Chem. Eng. J., 192 (2012) 171–178.
[25] J. Wang, X.Y. Wang, GPCC catalyzed hydrogen peroxide for decolorization of C.I. Reactive Red 24 from simulated dyeing wastewater, Water Sci. Technol., 82 (2020) 2381–2388.
[26] X. Wang, J. Gao, Absorption spectra of gelatin copper complexes and copper(II) sulfate and their impact on cotton peroxide bleaching, J. Nat. Fibers, 16 (2019) 307–318.
[27] X. Wang, J. Tang, An evaluation of the effectiveness of applying a gelatin–copper complex in the low-temperature bleaching of cotton with hydrogen peroxide, Color. Technol., 133 (2017) 300–304.
[28] X. Wang, C. Lu, C. Chen, Effect of chicken-feather protein-based flame retardant on flame retarding performance of cotton fabric, J. Appl. Polym. Sci., 131 (2014) 40584, doi: 10.1002/app.40584.
[29] M. Černík, V.V. Thekkae Padil, Green synthesis of copper oxide nanoparticles using gum karaya as a biotemplate and their antibacterial application, Int. J. Nanomed., 8 (2013) 889–898.
[30] Y. Amelkovich, O. Nazarenko, A. Sechin, P. Visakh, Characterization of copper nanopowders after natural aging, IOP Conf. Ser.: Mater. Sci. Eng., 81 (2015) 1–6.
[31] W. Chen, X. Feng, D. Zhang, F. Lu, H. Wang, J. Tan, Q. Xu, Y. Liu, Z. Cao, X. Su, In situ synthesis of $TiO_2$/NC on cotton fibers with antibacterial properties and recyclable photocatalytic degradation of dyes, RSC Adv., 12 (2022) 19974–19980.
[32] B. Bianco, I. De Michelis, F. Vegliò, Fenton treatment of complex industrial wastewater: optimization of process conditions by surface response method, J. Hazard. Mater., 186 (2011) 1733–1738.
[33] M. Munoz, G. Pliego, Z.M. de Pedro, J.A. Casas, J.J. Rodriguez, Application of intensified Fenton oxidation to the treatment of sawmill wastewater, Chemosphere, 109 (2014) 34–41.
[34] W. Yuan, C. Zhang, H. Wei, Q. Wang, K. Li, *In-situ* synthesis and immobilization of a Cu(II)–pyridyl complex on silica microspheres as a novel Fenton-like catalyst for RHB degradation at near-neutral pH, RSC Adv., 7 (2017) 22825–22835.
[35] L. Zhou, Z. Xu, J. Zhang, Z. Zhang, Y. Tang, Degradation of hydroxypropyl guar gum at wide pH range by a heterogeneous Fenton-like process using bentonite-supported Cu(0), Water Sci. Technol., 82 (2020) 1635–1642.
[36] D. Güçlü, N. Şirin, S. Şahinkaya, M.F. Sevimli, Advanced treatment of coking wastewater by conventional and modified Fenton processes, Environ. Prog. Sustainable Energy, 32 (2013) 176–180.
[37] Z. Hui, F. Hao, W. Yan, C. Lu, Decolorization of orange II by heterogeneous Fenton process using goethite as catalyst, Environ. Eng. Manage. J., 14 (2015) 737–744.
[38] D. Yuan, C. Zhang, S. Tang, Z. Wang, Q. Sun, X. Zhang, T. Jiao, Q. Zhang, Ferric ion-ascorbic acid complex catalyzed calcium peroxide for organic wastewater treatment: optimized by response surface method, Chin. Chem. Lett., 32 (2021) 3387–3392.
[39] I. Gulkaya, G. Surucu, F. Dilek, Importance of $H_2O_2/Fe^{2+}$ ratio in Fenton's treatment of a carpet dyeing wastewater, J. Hazard. Mater., 136 (2016) 763–769.
[40] C.-Y. Chang, Y.-H. Hsieh, K.-Y. Cheng, L.-L. Hsieh, T.-C. Cheng, K.-S. Yao, Effect of pH on Fenton process using estimation of hydroxyl radical with salicylic acid as trapping reagent, Water Sci. Technol., 58 (2008) 873–879.
[41] J.F. Perez-Benito, Copper(II)-catalyzed decomposition of hydrogen peroxide: catalyst activation by halide ions, Monatsh. Chem., 132 (2001) 1477–1492.
[42] Z. Shan, M. Lu, L. Wang, B. MacDonald, J. MacInnis, M. Mkandawire, X. Zhang, K.D. Oakes, Chloride accelerated Fenton chemistry for the ultrasensitive and selective colorimetric detection of copper, Chem. Commun., 52 (2016) 2087–2090.
[43] H. Xu, M. Prasad, Y. Liu, Schorl: a novel catalyst in mineral-catalyzed Fenton-like system for dyeing wastewater discoloration, J. Hazard. Mater., 165 (2009) 1186–1192.
[44] R. Cao, J. Guo, X. Hua, Y. Xu, Investigation on decolorization kinetics and thermodynamics of lignocellulosic xylooligosaccharides by highly selective adsorption with Amberlite XAD-16N, Food Chem., 310 (2020) 125934, doi: 10.1016/j.foodchem.2019.125934.
[45] Y.H. Mao, Y. Guan, Q.K. Zheng, X.N. Feng, X.X. Wang, Adsorption thermodynamic and kinetic of disperse dye on cotton fiber modified with tolylene diisocyanate derivative, Cellulose, 18 (2011) 271–279.
[46] A.F. Bertea, R. Butnaru, R. Berariu, Reducing pollution in reactive cotton dyeing through wastewater recycling, Cellul. Chem. Technol., 47 (2017) 133–139.
[47] R. Yamaguchi, S. Kurosu, M. Suzuki, Y. Kawase, Hydroxyl radical generation by zero-valent iron/Cu (ZVI/Cu) bimetallic catalyst in wastewater treatment: heterogeneous Fenton/Fenton-like reactions by Fenton reagents formed in-situ under oxic conditions, Chem. Eng. J., 334 (2018) 1537–1549.
[48] N.K. Pandey, H.B. Li, L. Chudal, B. Bui, E. Amador, M.B. Zhang, H.M. Yu, M.L. Chen, X. Luo, W. Chen, Exploration of copper-cysteamine nanoparticles as an efficient heterogeneous Fenton-like catalyst for wastewater treatment, Mater. Today Phys., 22 (2022) 100587, doi: 10.1016/j.mtphys.2021.100587.
[49] L. Wang, Y. Miao, M. Lu, Z. Shan, S. Lu, J. Hou, Q. Yang, X. Liang, T. Zhou, D. Curry, Chloride-accelerated Cu-Fenton chemistry for biofilm removal, Chem. Commun., 53 (2017) 5862–5865.
[50] H. Lee, J. Seong, K.-M. Lee, H.-H. Kim, J. Choi, J.-H. Kim, C. Lee, Chloride-enhanced oxidation of organic contaminants by Cu(II)-catalyzed Fenton-like reaction at neutral pH, J. Hazard. Mater., 344 (2018) 1174–1180.